

Phonon scattering in graphene over substrate steps

H. Sevinçli and M. Brandbyge

Citation: [Applied Physics Letters](#) **105**, 153108 (2014); doi: 10.1063/1.4898066

View online: <http://dx.doi.org/10.1063/1.4898066>

View Table of Contents: <http://scitation.aip.org/content/aip/journal/apl/105/15?ver=pdfcov>

Published by the [AIP Publishing](#)

Articles you may be interested in

[Resonant carrier-phonon scattering in graphene under Landau quantization](#)

Appl. Phys. Lett. **103**, 253117 (2013); 10.1063/1.4852635

[Electronic and phonon bandstructures of pristine few layer and metal doped graphene using first principles calculations](#)

AIP Advances **3**, 032117 (2013); 10.1063/1.4794949

[Low-temperature anomalies in the thermal conductivity of plastically deformed crystals caused by phonon-kink scattering](#)

Low Temp. Phys. **38**, 1055 (2012); 10.1063/1.4765094

[Wave packet simulations of phonon boundary scattering at graphene edges](#)

J. Appl. Phys. **112**, 024328 (2012); 10.1063/1.4740065

[Hydrogen vibrational modes on graphene and relaxation of the C–H stretch excitation from first-principles calculations](#)

J. Chem. Phys. **133**, 054505 (2010); 10.1063/1.3474806

An advertisement for Asylum Research Cypher AFMs. The background is dark blue with a glowing effect. On the left, there is a stylized image of a film strip and a purple, textured surface. The text is in white and orange. The main text reads: 'Not all AFMs are created equal', 'Asylum Research Cypher™ AFMs', and 'There's no other AFM like Cypher'. At the bottom, there is a website URL and the Oxford Instruments logo with the tagline 'The Business of Science®'.

Phonon scattering in graphene over substrate steps

H. Sevinçli^{1,2,a)} and M. Brandbyge^{2,3,b)}

¹Department of Materials Science and Engineering, Izmir Institute of Technology, Gülbahçe Kampüsü, 35430 Urla, Izmir, Turkey

²Department of Micro- and Nano-technology (DTU Nanotech), Technical University of Denmark, DK-2800 Kongens Lyngby, Denmark

³Center for Nanostructured Graphene (CNG), Department of Micro- and Nano-technology, Technical University of Denmark, DK-2800 Kongens Lyngby, Denmark

(Received 11 September 2014; accepted 2 October 2014; published online 15 October 2014)

We calculate the effect on phonon transport of substrate-induced bends in graphene. We consider bending induced by an abrupt kink in the substrate, and provide results for different step-heights and substrate interaction strengths. We find that individual substrate steps reduce thermal conductance in the range between 5% and 47%. We also consider the transmission across linear kinks formed by adsorption of atomic hydrogen at the bends and find that individual kinks suppress thermal conduction substantially, especially at high temperatures. Our analysis shows that substrate irregularities can be detrimental for thermal conduction even for small step heights. © 2014 AIP Publishing LLC.

[<http://dx.doi.org/10.1063/1.4898066>]

Graphene is the material with the highest thermal conductivity reported so far,^{1–3} with important prospective applications for example for thermal management of nano-electronics.^{4,5} The ultimately thin membrane adheres well to substrates and typically will ripple, wrinkle, and bubble form when graphene is transferred onto a flat substrate. On the other hand, since graphene is known to cling to the smallest irregularities,⁶ this also results in deformation and bending caused by the conformation of graphene to an irregular surface. This could, for instance, be steps in surfaces such as SiC or edges of other 2D materials such as BN. It is thus highly relevant to consider the effects of deformation on the thermal transport properties of graphene. There are several recent studies which investigate the effects of substrate induced geometrical modulations on the electronic and transport properties of graphene.^{7–10} In particular, Low and co-workers⁹ considered the effect on the electronic transport when graphene is deformed due to physisorption on a flat substrate presenting an abrupt step. They used a simple Lennard-Jones potential to model the substrate-graphene interaction with parameters corresponding to a step in SiC, and found that the bend itself causes an insignificant scattering of the electrons. Also, the related effect of ripples and wrinkles on electronic structure and transport in graphene on substrates has been investigated.^{11–13}

Inspired by the study of Low *et al.*,⁹ we here consider phonon transport for a model of an abrupt step in an otherwise structureless substrate. We calculate the transport for various step-heights and interaction strengths. The effects of the substrate are two-fold. First, (i) the geometry of graphene is modulated by the irregularity of the substrate, which alters the force constants locally and therefore scatters phonons. Second, (ii) the substrate gives rise to a renormalization of the vibrational modes and increases the line widths (i.e., reduces phonon lifetimes). Here, we focus on the

deformation (i) and neglect the dynamics of the structureless substrate.

We find that the effect of the substrate induced bend in the graphene on the phonon transport is not negligible, and can reduce the conductance with more than 10% at room temperature. For very strong substrate interaction, we obtain a decrease in phonon transmission comparable to that of a sp^3 kink-line induced by linear adsorption by hydrogen.^{10,14}

The graphene-substrate step model geometry studied here is shown in Fig. 1(a). The substrate is treated as a static continuum with an abrupt step at $x = 0$, parallel to the y -axis. We employ the density functional tight-binding (DFTB) method¹⁵ to describe graphene while the van der Waals (vdW) interaction between the sheet and the substrate is modelled with the 6–12 Lennard-Jones (LJ) potential $V_{LJ}(r) = 4\epsilon_{LJ}((\sigma/r)^{12} - (\sigma/r)^6)$.^{16,29} The direction transverse to the step (y) is described by periodic boundary conditions using 8 k_y -points in the DFTB force-constant calculations. The ends of the sheet are first left free to float at a fixed distance over the substrate, in order to find the correct bending geometry. Then, the ends are connected to semi-infinite graphene sheets which will serve as reservoirs in transport calculations. The minimum-energy geometries are calculated by minimizing the forces within a tolerance of 10^{-4} eV/Å. The force constant matrices are obtained by finite displacements of graphene atoms (10^{-2} Å) in each direction.¹⁷ An infinite mass is attributed to the substrate in order to disregard its dynamics. The phonon transmission was calculated using the Green's function method, see, e.g., Ref. 18, and averaged over 25 k_y -points.

We fix the substrate-graphene distance to 3.4 Å ($\sigma = 3.03$ Å) corresponding to the interlayer spacing in graphite and a typical interlayer distance for van der Waals heterolayers. The same distance is used for defining the cross sectional area for phonon transmission and conductance allowing for comparison with bulk 3D materials. We calculate the phonon transport for a variation of step heights ($h_s = 1, 5, 10, 20, 50$ Å). Following Low *et al.*,⁹ we use as a starting point $\epsilon_{LJ} = 40$ meV corresponding to a SiC

^{a)}Electronic mail: haldunsevincli@iyte.edu.tr

^{b)}Electronic mail: mads.brandbyge@nanotech.dtu.dk

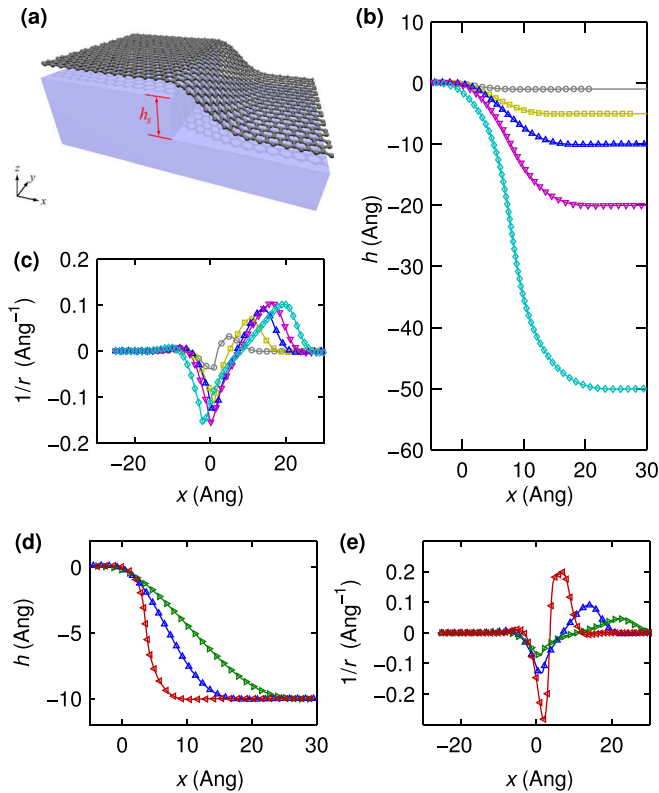


FIG. 1. (a) Illustration of graphene over a substrate step with height h_s . The step is located at $x=0$ and is parallel to the y -axis. The profile of the sheet on the xz -plane and the radius of curvature are plotted for $h_s = 1, 5, 10, 20$, and 50 \AA with $\epsilon_{LJ} = 40 \text{ meV}$ ((b) and (c)); and for $h_s = 10 \text{ \AA}$ with $\epsilon_{LJ} = 20, 40, 160 \text{ meV}$ ((d) and (e)).

substrate. However, adhesion energy of graphene display a large variation depending on the substrate. On insulating surfaces, the estimations for the binding energy per carbon atom ranges from 10 to 77 meV.^{6,19–23} On metallic substrates, density functional theory suggests that it can be as high as 327 meV.^{24–26} We choose $\epsilon_{LJ} = 20, 40$, and 160 meV with $h_s = 10 \text{ \AA}$ to address the effects of the coupling strength.

Bending profiles are plotted for various step heights with $\epsilon_{LJ} = 40 \text{ meV}$ (Fig. 1(b)) and for $h_s = 10 \text{ \AA}$ with $\epsilon_{LJ} = 20, 40$, and 160 meV (Fig. 1(d)), and the corresponding inverse radii of curvature $1/r$ are plotted in Figs. 1(c) and 1(e). Varying h_s from 1 to 50 \AA , the minimum values of r range between 25 and 6.3 \AA at the upper edge, and between 31.3 to 9.6 \AA at the lower edge, and the change in r is significantly slower when $h_s \geq 10 \text{ \AA}$. For a step height of 10 \AA , we find that the minimum radius of curvature r is $13.5, 7.7$, and 3.3 \AA ($21.7, 10.9$, and 5 \AA) for $\epsilon_{LJ} = 20, 40$, and 160 meV at the upper (lower) edge, respectively. These values are in agreement with those in Ref. 9.

Phonon transmission spectra per cross section are shown in Fig. 2. In Fig. 2(a), we consider the transmission spectra of flat graphene for varying ϵ_{LJ} . The out-of-plane acoustic modes gain a gap at zero energy since the translational symmetry is broken in the z -direction, the size of the gap increases with the square-root of ϵ_{LJ} . Besides this, the substrate does not alter the transmission spectra of the flat graphene significantly. Keeping ϵ_{LJ} constant at 40 meV , the effect of varying h_s on transmission is plotted in Fig. 2(b). The effect of the step on the transmission is most pronounced

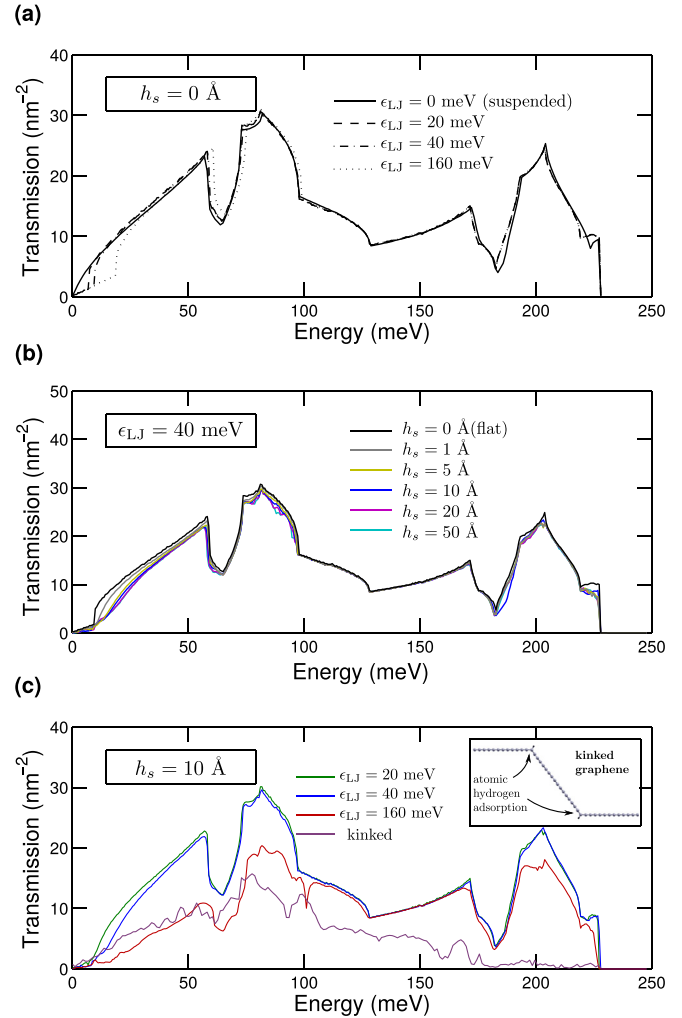


FIG. 2. Transmission per cross section area for various structures. The effect of substrate coupling in the absence of a step height for different coupling strengths are given in (a). Transmission with varying the step height, h_s , for fixed coupling strength $\epsilon_{LJ} = 40 \text{ meV}$ (b), and with varying the coupling strength for a fixed step height $h_s = 10 \text{ \AA}$ (c).

at the lower vibrational energies. As is the case for the minimum r , the transmission spectra are also less sensitive to h_s when it is greater than 10 \AA , but it is quite sensitive to the interaction strength. In Fig. 2(c), we plot transmission for $h_s = 10 \text{ \AA}$ and different ϵ_{LJ} , namely $20, 40$, and 160 meV . The effect of the step when $\epsilon_{LJ} = 20 \text{ meV}$ is relatively small, but it is substantial for $\epsilon_{LJ} = 160 \text{ meV}$.

We also consider the effect of kinks on phonon transport. Since bending increases the chemical reactivity of graphene sheet, linear kinks can be produced by adsorption of atomic hydrogen at the step edges.^{27,28} Hydrogen adsorption not only modifies the hybridization but also bends the sheet abruptly with a vanishingly small radius of curvature, i.e., generates a kink, see Fig. 2(c), inset. Due to the sp^3 bonding, kinks were predicted to form efficient barriers for electron transmission.¹⁰ The case is similar for phonons. In Fig. 2(c), the phonon transmission spectrum of graphene with double kinks at the upper and lower edges of the step with $h_s = 17 \text{ \AA}$ is also plotted. The phonon transmission is severely altered due to kinks. In the case of smooth bends, transmission is mostly affected at lower energies, while in the kinked case, higher frequency phonons are also strongly suppressed.

Thermal conductance per cross section is calculated as

$$\kappa = \frac{k_B}{2\pi} \int d\omega p(\omega, T) \mathcal{T}(\omega), \quad (1)$$

with k_B being the Boltzmann constant, T temperature, and \mathcal{T} the transmission per cross section. The weight function is $p = -x^2 \partial f_B / \partial x$ with $x = \hbar\omega / k_B T$ and $f_B = (e^x - 1)^{-1}$ being the Bose function. We note that p has its peak value ($p = 1$) at $x = 0$, and half-maximum at $x \approx 2.983$. That is, at room temperature, most of the contribution is due to phonons with $\hbar\omega < 75$ meV. For this reason, the substrate induced energy gap of out-of-plane modes are not affecting the room temperature properties dramatically. We find a significant reduction of conductance due to the finite step heights (Fig. 3). For $h_s = 10 \text{ \AA}$, and $\epsilon_{LJ} = 40$ meV, κ is reduced by 44%, 11%, 8%, and 7% at 50 K, 300 K, 500 K, and 1000 K, respectively. For $h_s = 1 \text{ \AA}$ (50 \AA), the reductions are 22%, 5%, 4%, and 4% (47%, 12%, 10%, and 9%). Depending on the interaction strength, κ is reduced by 5%, 11%, and 47% at room temperature for $\epsilon_{LJ} = 20$ meV, 40 meV, and 160 meV, respectively.

In Fig. 4(a), we plot the ratio of thermal conductance of graphene over a step to that of flat graphene with

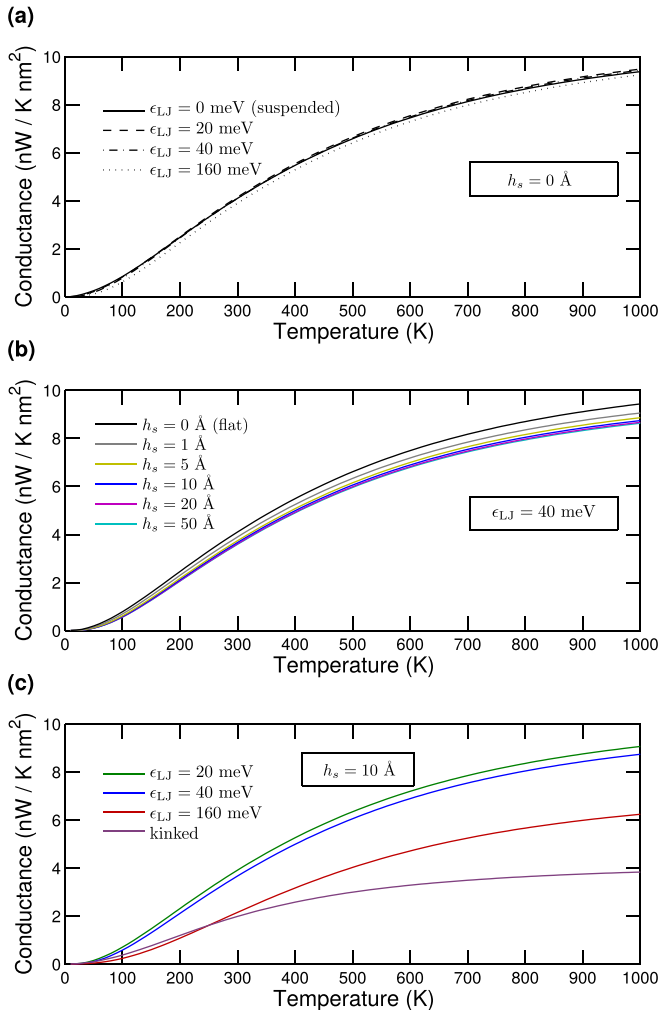


FIG. 3. Thermal conductance per cross section area (a) for flat graphene with different strengths of substrate interaction, (b) for different step heights with a fixed interaction strength ($\epsilon_{LJ} = 40$ meV), (c) for different interaction strengths and a fixed step height ($h_s = 10 \text{ \AA}$). Thermal conductance of kinked graphene is also shown for comparison.

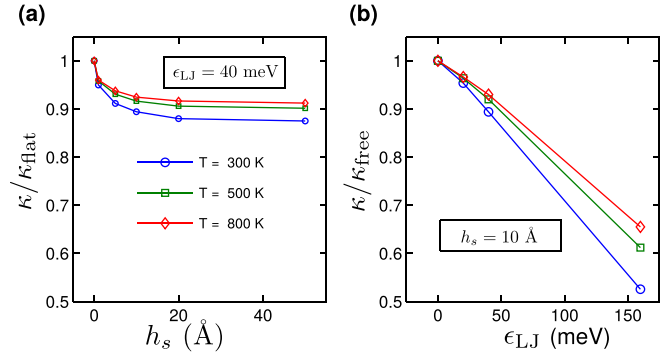


FIG. 4. The ratio of thermal conductance of graphene over a step for a fixed interaction strength ($\epsilon_{LJ} = 40$ meV) as a function of the step height (a), and for a fixed step height ($h_s = 10 \text{ \AA}$) as a function of the interaction strength (b).

$\epsilon_{LJ} = 40$ meV. Even a small step of 1 \AA reduces κ by approximately 5%, while the reduction saturates at around 10% for higher steps. On the other hand, keeping $h_s = 10 \text{ \AA}$, the ratio of κ to that of free standing graphene is sensitive to the coupling strength as seen in Fig. 4(b). The thermal resistance of a step can be defined as $R_s = \kappa^{-1} - \kappa_{\text{flat}}^{-1}$. At 300 K, $R_s = 0.013$ (0.035) $\text{nm}^2 \text{ K/nW}$ for $h_s = 1$ (50) \AA and $\epsilon_{LJ} = 40$ meV, where $\kappa_{\text{flat}}^{-1} = 0.243 \text{ nm}^2 \text{ K/nW}$. Assuming that resistance due to individual steps are additive, one concludes that only a small number of substrate steps can reduce the thermal conductivity by a substantial amount and thus play a major role for thermal transport in graphene when supported by a substrate.

We thank Peter Bøggild and Jesper T. Rasmussen for fruitful discussions. H.S. acknowledges support from Danish Council for Independent Research, Individual Postdoc Grant (No. 0602-02477B-FTP), from Scientific and Research Council of Turkey, TÜBİTAK (BİDEB-113C032), and from Bilim Akademisi—the Science Academy, Turkey under the BAGEP program. We also would like to thank TÜBİTAK ULAKBİM High Performance Computing Center.

- ¹A. A. Balandin, S. Ghosh, W. Bao, I. Calizo, D. Teweldebrhan, F. Miao, and C. N. Lau, *Nano Lett.* **8**, 902 (2008).
- ²A. Balandin, *Nat. Mater.* **10**, 569 (2011).
- ³D. L. Nika and A. A. Balandin, *J. Phys.: Condens. Matter* **24**, 233203 (2012).
- ⁴S. Ghosh, I. Calizo, D. Teweldebrhan, E. P. Pokatilov, D. L. Nika, A. A. Balandin, W. Bao, F. Miao, and C. N. Lau, *Appl. Phys. Lett.* **92**, 151911 (2008).
- ⁵K. M. F. Shahil and A. A. Balandin, *Solid State Commun.* **152**, 1331 (2012).
- ⁶J. S. Bunch and M. L. Dunn, *Solid State Commun.* **152**, 1359 (2012).
- ⁷J.-K. Lee, S. Yamazaki, H. Yun, J. Park, G. P. Kennedy, G.-T. Kim, O. Pietzsch, R. Wiesendanger, S. Lee, S. Hong, U. Dettlaff-Weglikowska, and S. Roth, *Nano Lett.* **13**, 3494 (2013).
- ⁸J. Hicks, A. Tejada, A. Taleb-Ibrahimi, M. S. Nevius, F. Wang, K. Shepperd, J. Palmer, F. Bertran, P. Le Fèvre, J. Kunc, W. A. de Heer, C. Berger, and E. H. Conrad, *Nat. Phys.* **9**, 49 (2013).
- ⁹T. Low, V. Perebeinos, J. Tersoff, and P. Avouris, *Phys. Rev. Lett.* **108**, 096601 (2012).
- ¹⁰J. T. Rasmussen, T. Gunst, P. Bøggild, A.-P. Jauho, and M. Brandbyge, *Beilstein J. Nanotechnol.* **4**, 103 (2013).
- ¹¹W. Bao, F. Miao, Z. Chen, H. Zhang, W. Jang, C. Dames, and C. N. Lau, *Nat. Nanotechnol.* **4**, 562 (2009).
- ¹²R. Miranda and A. L. Vázquez de Parga, *Nat. Nanotechnol.* **4**, 549 (2009).
- ¹³Z. Pan, N. Liu, L. Fu, and Z. Liu, *J. Am. Chem. Soc.* **133**, 17578 (2011).

- ¹⁴L. A. Chernozatonskii, P. B. Sorokin, and J. W. Brüning, *Appl. Phys. Lett.* **91**, 183103 (2007).
- ¹⁵B. Aradi, B. Hourahine, and T. Frauenheim, *J. Phys. Chem. A* **111**, 5678 (2007).
- ¹⁶There are other potentials available for modelling inter-layer interactions, like the spherically symmetric inter-atomic potential used in Ref. 29. Since the scope of the present study is the effects of a generic substrate, we limit our discussion to Lennard-Jones potential only.
- ¹⁷A. Togo, F. Oba, and I. Tanaka, *Phys. Rev. B* **78**, 134106 (2008).
- ¹⁸H. Sevinçli, C. Sevik, T. Çağın, and G. Cuniberti, *Sci. Rep.* **3**, 1228 (2013).
- ¹⁹A. Mattausch and O. Pankratov, *Phys. Rev. Lett.* **99**, 076802 (2007).
- ²⁰M. Z. Hossain, *Appl. Phys. Lett.* **95**, 143125 (2009).
- ²¹Z. Ao, M. Jiang, Z. Wen, and S. Li, *Nanoscale Res. Lett.* **7**, 158 (2012).
- ²²Y.-J. Kang, J. Kang, and K. J. Chang, *Phys. Rev. B* **78**, 115404 (2008).
- ²³T. C. Nguyen, M. Otani, and S. Okada, *Phys. Rev. Lett.* **106**, 106801 (2011).
- ²⁴T. Yoon, W. C. Shin, T. Y. Kim, J. H. Mun, T.-S. Kim, and B. J. Cho, *Nano Lett.* **12**, 1448 (2012).
- ²⁵P. A. Khomyakov, G. Giovannetti, P. C. Rusu, G. Brocks, J. van den Brink, and P. J. Kelly, *Phys. Rev. B* **79**, 195425 (2009).
- ²⁶M. Vanin, J. J. Mortensen, A. K. Kelkkanen, J. M. Garcia-Lastra, K. S. Thygesen, and K. W. Jacobsen, *Phys. Rev. B* **81**, 081408 (2010).
- ²⁷D. Srivastava, D. W. Brenner, J. D. Schall, K. D. Ausman, M. Yu, and R. S. Ruoff, *J. Phys. Chem. B* **103**, 4330 (1999).
- ²⁸D. C. Elias, R. R. Nair, T. M. G. Mohiuddin, S. V. Morozov, P. Blake, M. P. Halsall, A. C. Ferrari, D. W. Boukhvalov, M. I. Katsnelson, A. K. Geim, and K. S. Novoselov, *Science* **323**, 610 (2009).
- ²⁹D. L. Nika, A. I. Cocemasov, and A. A. Balandin, *Appl. Phys. Lett.* **105**, 031904 (2014).